

**Compressibility of  $CeMIn_5$  and  $Ce_2MIn_8$  ( $M=Rh, Ir, \text{ and } Co$ ) compounds**

Ravhi S. Kumar and A. L. Cornelius

*Department of Physics, University of Nevada, Las Vegas, Nevada 89154-4002, USA*

J. L. Sarrao

*Materials Science and Technology Division, Los Alamos National Laboratory, Los Alamos, New Mexico 87545, USA*

(Received 3 May 2004; revised manuscript received 27 September 2004; published 29 December 2004)

The lattice parameters of the tetragonal compounds  $CeMIn_5$  and  $Ce_2MIn_8$  ( $M=Rh, Ir, \text{ and } Co$ ) have been studied as a function of pressure up to 15 GPa using a diamond anvil cell under both hydrostatic and quasi-hydrostatic conditions at room temperature. The addition of  $MIn_2$  layers to the parent  $CeIn_3$  compound is found to stiffen the lattice as the 2-layer systems (average of bulk modulus values  $B_0$  is 70.4 GPa) have a larger  $B_0$  than  $CeIn_3$  (67 GPa), while the 1-layer systems are even stiffer (average of  $B_0$  is 81.4 GPa). Estimating the hybridization using parameters from tight binding calculations shows that the dominant hybridization is  $fp$  in nature between the Ce and In atoms. The values of  $V_{pf}$  at the pressure where the superconducting transition temperature  $T_c$  reaches a maximum is the same for all  $CeMIn_5$  compounds. By plotting the maximum values of the superconducting transition temperature  $T_c$  versus  $c/a$  for the studied compounds and Pu-based superconductors, we find a universal  $T_c$  versus  $c/a$  behavior when these quantities are normalized appropriately. These results are consistent with magnetically mediated superconductivity.

DOI: 10.1103/PhysRevB.70.214526

PACS number(s): 61.10.Nz, 62.50.+p, 51.35.+a, 71.27.+a

**I. INTRODUCTION**

Ce based heavy fermion (HF) and antiferromagnetic (AF) compounds have been the subject of intensive investigations due to their unconventional magnetic and superconducting properties. In these compounds the electronic correlations, the magnetic ordering temperature and the crystal field effects are sensitive to pressure, and pressure induced superconductivity near a quantum critical point (QCP) has been observed in a variety of compounds such as  $CePd_2Si_2$ ,  $CeCu_2Ge_2$ ,  $CeRh_2Si_2$  and  $CeIn_3$ .<sup>1-5</sup> The appearance of superconductivity in these systems and the deviation from Fermi liquid behavior as a function of pressure are still challenging problems to be studied.

$Ce_nMIn_{2n+3}$  ( $M=Rh, Ir, \text{ and } Co$ ) with  $n=1$  or 2 crystallize in the quasi-two-dimensional (quasi-2D) tetragonal structures  $Ho_nCoGa_{2n+3}$ .<sup>6,7</sup> The crystal structure can be viewed as  $(CeIn_3)_n(MIn_2)$  with alternating  $n$  ( $CeIn_3$ ) and  $(MIn_2)$  layers stacked along the  $c$ -axis. By looking at the crystal structure, we would expect that AF correlations would develop in the cubic ( $CeIn_3$ ) layers in a manner similar to bulk  $CeIn_3$ .<sup>8</sup> The AF ( $CeIn_3$ ) layers will then be weakly coupled by an inter-layer exchange interaction through the  $(MIn_2)$  layer leading to a quasi-2D magnetic structure. Indeed, in the Rh compounds, the magnetic properties, as determined by thermodynamic,<sup>9</sup> NQR,<sup>10</sup> and neutron scattering<sup>11</sup> are less 2D as the crystal structure becomes less 2D going from single layer  $CeRhIn_5$  to double layer  $Ce_2RhIn_8$  (note that as  $n \rightarrow \infty$ , one gets the 3D cubic system  $CeIn_3$ ).  $CeRhIn_5$  and  $Ce_2RhIn_8$  are antiferromagnets at ambient pressure but are found to superconduct at high pressures.<sup>12-15</sup> The systems  $CeCoIn_5$ ,  $CeIrIn_5$ , and  $Ce_2CoIn_8$  display superconductivity at ambient pressure.<sup>13,14,16-18</sup> The only member of the series that does not display magnetic order or superconductivity at ambient pressures is  $Ce_2IrIn_8$  that is believed to be near a QCP.<sup>19</sup>

While not proven definitively, it is generally believed that the origin of the superconductivity in  $Ce_nMIn_{2n+3}$  is magnetic in origin. The value of the superconducting transition temperature  $T_c$  in magnetically mediated superconductors is believed to be dependent on dimensionality in addition to the characteristic spin fluctuation temperature. Theoretical models and experimental results suggest that the SC state in  $CeRhIn_5$  may be due to the quasi-two-dimensional (2D) structure and anisotropic AF fluctuations which are responsible for the enhancement of  $T_c$  relative to  $CeIn_3$ .<sup>20,21</sup> A strong correlation between the ambient pressure ratio of the tetragonal lattice constants  $c/a$  and  $T_c$  in the  $CeMIn_5$  compounds is indicative of the enhancement of the superconducting properties by lowering dimensionality (increasing  $c/a$  increases  $T_c$ ).<sup>20</sup> In order to explain the evolution of superconductivity induced by pressure and the suppression of AF ordering, it is important to probe the effect of pressure on structure for these compounds and look for possible correlations between structural and thermodynamic properties.

Here we report on high pressure x-ray diffraction measurements performed on  $Ce_nMIn_{2n+3}$  ( $M=Rh, Ir \text{ and } Co$ ) with  $n=1$  or 2 up to 15 GPa under both hydrostatic and quasihydrostatic conditions. Previously, we have reported results on  $CeRhIn_5$ ;<sup>22</sup> we present a comparative study of the complete set of  $Ce_nMIn_{2n+3}$  compounds with emphasis on the behavior near the QCP. While there is no direct correlation between  $c/a(P)$  and  $T_c(P)$  as an implicit function of pressure in an individual system, the value of  $c/a$  at the pressure where  $T_c$  reaches its maximum value DOES show linear behavior as previously hypothesized.<sup>20</sup> Also, the  $pf$  hybridization  $V_{pf}$  between the Ce and In atoms is the dominant hybridization in these compounds and takes on the same value for all  $CeMIn_5$  compounds at the pressure  $P_{max}$  where  $T_c$  reaches its maximum value. These results will be compared to isostructural Pu compounds and all of the results are

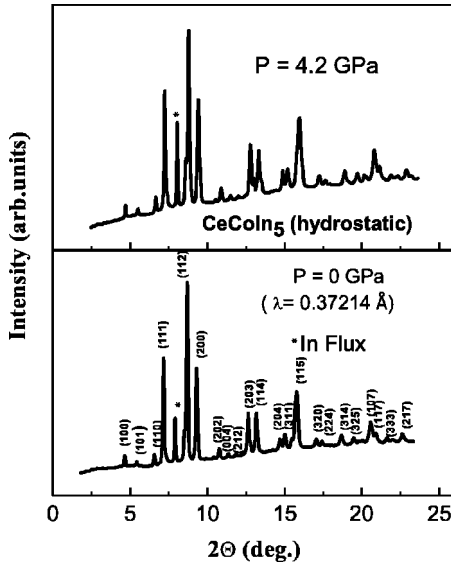


FIG. 1. X-ray diffraction patterns of CeCoIn<sub>5</sub> at ambient pressure and a hydrostatic pressure of 4.2 GPa. The data were taken using synchrotron radiation of wavelength  $\lambda=0.37214$  Å. The various reflections from CeCoIn<sub>5</sub> are labeled and one peak due to excess In flux is noted.

consistent with unconventional, magnetically mediated superconductivity.

## II. EXPERIMENT

Ce<sub>n</sub>MIn<sub>2n+3</sub> single crystals were grown by a self-flux technique described elsewhere.<sup>23</sup> The single crystals were crushed into powder and x-ray diffraction measurements show the single phase nature of the compound. In agreement with previous results,<sup>23,24</sup> the crystals were found to have tetragonal symmetry with cell parameters in agreement with literature values.

The high pressure x-ray diffraction (XRD) experiments were performed using a rotating anode x ray generator (Rigaku) for the quasihydrostatic runs and synchrotron x-rays at HPCAT, Sector 16 at the Advanced Photon Source for hydrostatic measurements. The sample was loaded with NaCl or ruby powder as a pressure calibrant and either a silicone oil or 4:1 methanol:ethanol mixture (hydrostatic) or NaCl (quasihydrostatic) as the pressure transmitting medium in a Re gasket with a 180  $\mu\text{m}$  diameter hole. High pressure was achieved using a Merrill-Basset diamond anvil cell with 600  $\mu\text{m}$  culet diameters. The XRD patterns are collected using an imaging plate (300  $\times$  300 mm<sup>2</sup>) camera with 100  $\times$  100  $\mu\text{m}^2$  pixel dimensions. XRD patterns were collected up to 15 GPa at room ( $T=295$  K) temperature. The images were integrated using FIT2D software.<sup>25</sup> The structural refinement of the patterns was carried out using the Rietveld method on employing the FULLPROF and REITICA (LHPM) software packages.<sup>26</sup>

## III. RESULTS AND DISCUSSION

In Fig. 1 we show the XRD patterns for CeCoIn<sub>5</sub> obtained

at ambient pressure and a hydrostatic pressures of 4.2 GPa with silicone oil used as the pressure transmitting media. In other measurements, diffraction peaks from the Re gasket, pressure markers (NaCl) and the sample are all observed. The known equation of state for NaCl<sup>27</sup> or the standard ruby fluorescence technique<sup>28</sup> was used to determine the pressure. The refinement of the XRD patterns was performed on the basis of the Ho<sub>n</sub>CoGa<sub>2n+3</sub> structure with the  $P4/mmm$  space group (No. 123). When comparing the crystallographic data and bulk modulus of CeIn<sub>3</sub> relative to Ce<sub>n</sub>MIn<sub>2n+3</sub> it is evident that the Ce atom in Ce<sub>n</sub>MIn<sub>2n+3</sub> experiences a chemical pressure at ambient conditions,<sup>9,12</sup> leading one to expect the Ce<sub>n</sub>MIn<sub>2n+3</sub> to be less compressible than CeIn<sub>3</sub> as the bulk modulus increases with increasing pressure.

The  $V(P)$  data have been plotted in Fig. 2 for CeMIn<sub>5</sub> ( $M=\text{Rh, Ir, and Co}$ ) and Fig. 3 for Ce<sub>2</sub>MIn<sub>8</sub> ( $M=\text{Rh or Ir}$ ) for both quasihydrostatic and hydrostatic measurements (the data for CeRhIn<sub>8</sub> has been previously reported<sup>22</sup>). Note that the vertical and horizontal scales are the same for all graphs. Unfortunately, we have not had success growing single crystals of Ce<sub>2</sub>CoIn<sub>8</sub>, though others have reported successful growth of single crystals.<sup>18</sup> Since the maximum volume compression is only of the order of 10%, the  $V(P)$  data has been fit using a least squares fitting procedure to the first order Murnaghan equation of state

$$P = \frac{B_0}{B'_0} \left[ \left( \frac{V_0}{V(P)} \right)^{B'_0} - 1 \right], \quad (1)$$

where  $B_0$  is the initial bulk modulus and  $B'_0$  is the pressure derivative of  $B_0$ . For the room temperature ( $T=295$  K) data  $V/V_0$  data shown in Figs. 2 and 3, the values of  $B_0$  and  $B'_0$  and the initial linear compressibilities  $\kappa_a$  and  $\kappa_c$  calculated below 2 GPa are given in Table I. First, we note that the  $n=2$  compounds show more anisotropy ( $\kappa_a$  is 15–20% smaller than  $\kappa_c$ ) in the the compressibilities than the  $n=1$  compounds. As mentioned, the  $n=1$  compounds appear to be more 2D than the  $n=2$  compounds, making this result somewhat surprising. We also note the deviation from the typical inverse relationship between  $B_0$  and  $V_0$ ; namely, CeIrIn<sub>5</sub> has the largest value of  $B_0$  and the largest ambient pressure volume. These results hint that the valence of Ce and hybridization between the Ce 4*f* electrons and the conduction electrons needs to be taken into account. Pressure is known to make Ce compounds more tetravalent, and since the tetravalent ion is smaller than the trivalent ion, makes the more tetravalent system less compressible. The explanation for the unexpected difference in the linear compressibilities may lie in the fact that  $c/a$  seems to be coupled to  $T_c$  as will be discussed later. As a larger  $c/a$  favors superconductivity, if pressure reduces  $c$  less than expected, the compressibility will be lowered and the  $c/a$  ratio will increase as seen in CeRhIn<sub>5</sub> and CeCoIn<sub>5</sub>. As expected, the lattice appears to be stiffer the more 2D the system becomes as the MIn<sub>2</sub> layers in Ce<sub>2</sub>MIn<sub>8</sub> stiffen the structure relative to CeIn<sub>3</sub>. CeIn<sub>3</sub> has a smaller bulk modulus ( $B_0=67$  GPa)<sup>29</sup> than the 2-layer systems (average of  $B_0$  is 70.4 GPa) that in turn is smaller than the 1-layer systems (average of  $B_0$  is 81.4 GPa). The bulk modulus values compare well with those reported for other

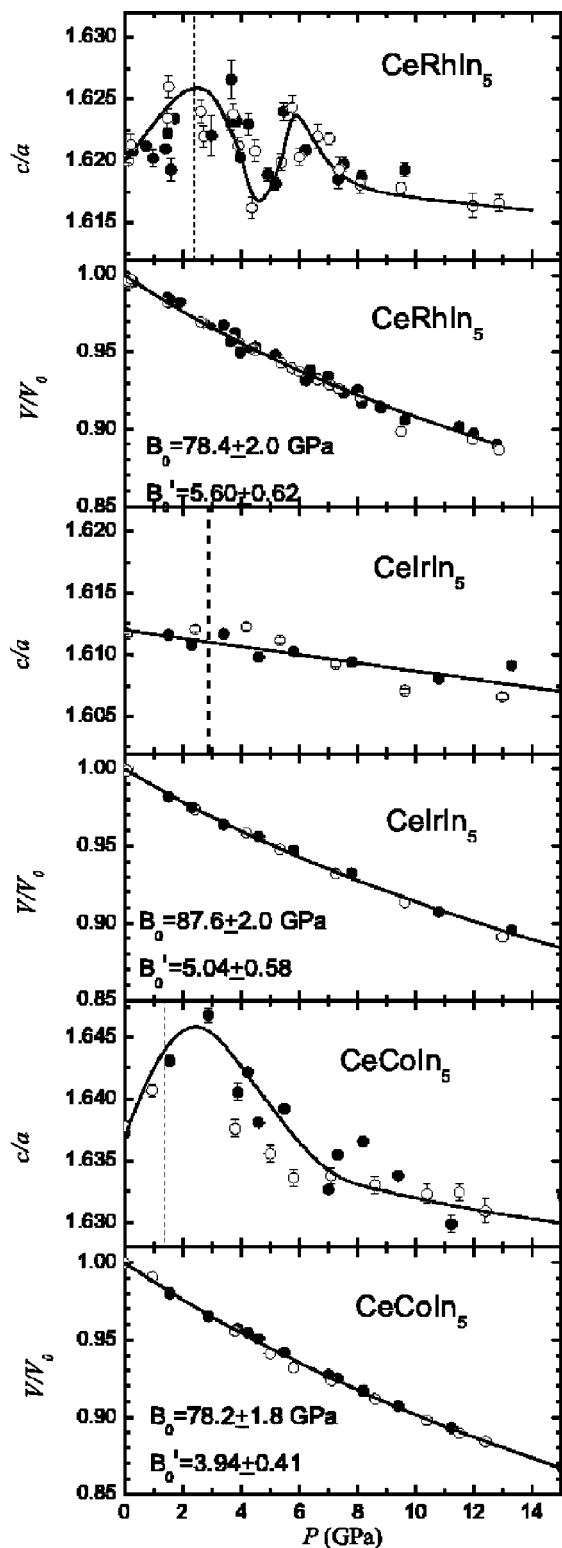


FIG. 2. Normalized volume  $V/V_0$  and ratio of tetragonal lattice constants  $c/a$  plotted versus pressure for CeMIn<sub>5</sub> compounds at room temperature. Data for both quasi-hydrostatic (open symbols) and hydrostatic (closed symbols) are displayed. The solid line through the volume data is a fit as described in the text. The dashed vertical lines in the  $c/a$  plots show the pressure where the maximum value of  $T_c$  is observed. The solid lines in the  $c/a$  plots are guides for the eye.

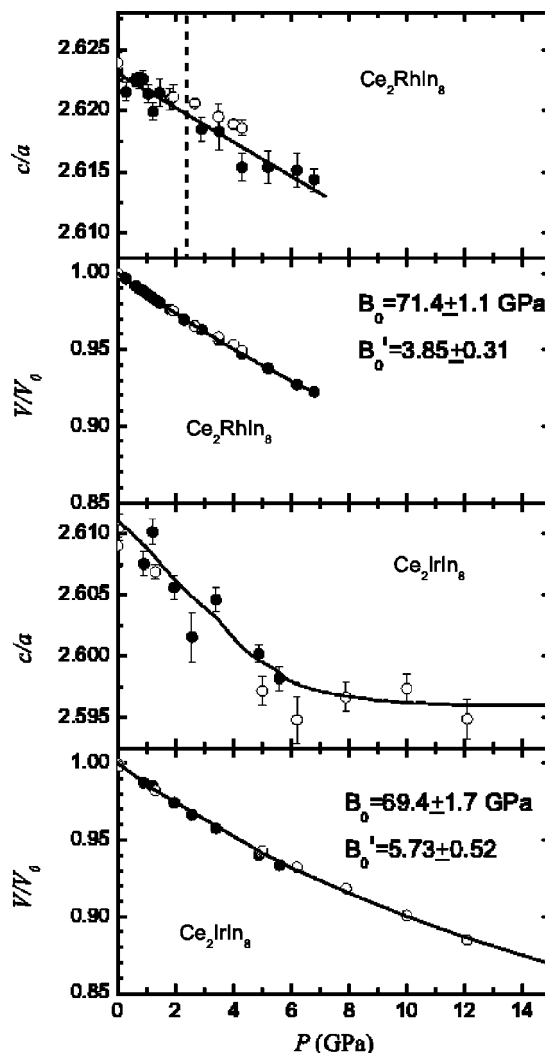


FIG. 3. Normalized volume  $V/V_0$  and ratio of tetragonal lattice constants  $c/a$  plotted versus pressure for Ce<sub>2</sub>MIn<sub>8</sub> compounds at room temperature. Data for both quasi-hydrostatic (open symbols) and hydrostatic (closed symbols) are displayed. The solid line through the volume data is a fit as described in the text. The dashed vertical lines in the  $c/a$  plots show the pressure where the maximum value of  $T_c$  is observed. The solid lines in the  $c/a$  plots are guides for the eye.

HF systems.<sup>30–33</sup> The fact that we see no discernible difference between the hydrostatic and quasi-hydrostatic measurements is likely due to the nearly isotropic compressibilities.

Figures 2 and 3 also show the ratio of the lattice constants  $c/a$  as a function of pressure. The systems display a wide range of behavior from the apparent double peaked structure in CeRhIn<sub>5</sub> to the single peaked structure in CeCoIn<sub>5</sub> to a monotonic decrease for the other systems. Vertical dashed lines show the pressure where a maximum in  $T_c(P)$  has been observed: 2.4 GPa for CeRhIn<sub>5</sub>,<sup>12,14</sup> 1.4 GPa for CeCoIn<sub>5</sub>,<sup>34,35</sup> 2.9 GPa for CeIrIn<sub>5</sub>,<sup>36</sup> and 2.4 GPa for Ce<sub>2</sub>RhIn<sub>8</sub>.<sup>15</sup>

As mentioned, a strong correlation between the ambient pressure  $c/a$  ratio and  $T_c$  in the CeMIn<sub>5</sub> compounds has been observed (increasing  $c/a$  increases  $T_c$ ).<sup>20</sup> This can be seen in Fig. 4 that is adapted from Pagliuso *et al.*<sup>20</sup> (Note that we

TABLE I. Summary of the determined bulk modulus  $B_0$  and its pressure derivative  $B'_0$  as determined from fits to the Murnaghan equation for the  $Ce_nMIn_{2n+3}$  compounds. Also listed are the ambient pressure values of  $V_0$  and  $c/a$  along with the initial linear compressibilities  $\kappa_a$  and  $\kappa_c$ . Values for  $CeIn_3$  are taken from Vedel *et al.* (Ref. 29).

System	$n$	$V_0$ ( $\text{\AA}^3$ )	$c/a$	$B_0$ (GPa)	$B'_0$	$\kappa_a(10^{-3} \text{ GPa}^{-1})$	$\kappa_c(10^{-3} \text{ GPa}^{-1})$
CeRhIn <sub>5</sub>	1	163.03	1.621	78.4±2.0	5.60±0.62	3.96±0.08	4.22±0.10
CeIrIn <sub>5</sub>	1	163.67	1.612	87.6±2.0	5.04±0.58	3.44±0.06	3.48±0.08
CeCoIn <sub>5</sub>	1	160.96	1.638	78.2±1.8	3.94±0.41	4.35±0.08	3.43±0.16
Ce <sub>2</sub> RhIn <sub>8</sub>	2	266.48	2.624	71.4±1.1	3.85±0.31	4.20±0.04	4.85±0.11
Ce <sub>2</sub> IrIn <sub>8</sub>	2	266.26	2.610	69.4±1.7	5.73±0.52	4.02±0.06	4.93±0.12
CeIn <sub>3</sub>	$\infty$	103.10	1	67.0±3.0	2.5±0.5	4.98±0.13	4.98±0.13

have corrected a labeling error found in Pagliuso *et al.*<sup>20</sup> where two systems are labeled as  $CeCo_{0.5}Ir_{0.5}In_5$ .) However, some discrepancies exist, namely magnetic systems like CeRhIn<sub>5</sub> whose  $c/a$  ratio of 1.62 would lead one to erroneously conclude that superconductivity near 1.0 K should be observed, rather than the experimentally observed AF order at 3.8 K. The reason for this discrepancy can be seen if one considers theoretical treatments of magnetically mediated superconductivity.<sup>21</sup> Calculations show that superconductivity occurs at a QCP where long range magnetic order is suppressed and the infinite range magnetic correlations give way to short range magnetic correlations that are responsible for the superconductivity. Recent work has shown a similar sort of behavior when a system is near a valence instability and critical density fluctuations give rise to superconductivity.<sup>37</sup> In either of these scenarios, one then finds  $T_c(P)$  behavior that displays the experimentally observed inverse parabolic behavior with the maximum value of  $T_c$  becoming larger as correlations become more 2D in character. Slight deviations from the inverse parabolic behavior observed in CeRhIn<sub>5</sub> on the high pressure side<sup>38</sup> may be indicative of density fluctuations or a “hidden” 3D

magnetically ordered state.<sup>39</sup> In the magnetic fluctuation scenario, the maximum value of  $T_c(P)$  is found at a pressure  $P_{\max}$  and depends on the spin fluctuation temperature  $T_{sf}$  and the dimensionality of the magnetic interactions. The maximum possible values of  $T_c$  will occur for more 2D systems with the highest possible value of  $T_{sf}$ . This leads to the natural conclusion that the correct quantities to plot are not the ambient pressure ones, but rather the value of  $T_c$  at  $P_{\max}$  and the corresponding value of  $c/a$ . Note that while one should use the structural information near  $T_c$ , we have shown that the  $c/a$  versus  $P$  behavior is similar at room temperature and near  $T_c$  leading to the conclusion that the room temperature lattice constants can be used for our analysis.<sup>22</sup> This has been done in Fig. 4 where the filled circles correspond to the  $c/a$  ratios from the current study where  $T_c$  reaches its maximum value at  $P_{\max}$  taken from the literature.<sup>12,14,34–36</sup> As can be seen, CeRhIn<sub>5</sub> now fits in with the rest of the data quite well. Also, CeIrIn<sub>5</sub> and CeCoIn<sub>5</sub> both have their values of  $T_c$  and  $c/a$  enhanced from their ambient pressure values. Note that all of the points from the current study lie on or above the line. These results are consistent with theory and it would be of great interest to measure more values of the maximum  $T_c$  as a function of  $c/a$  at that pressure to look for universal behavior.

To conclude that the dependence of  $T_c$  on  $c/a$  in Fig. 4 is due mainly to dimensionality, it is necessary to prove that  $T_{sf}$  does not change drastically for the various compounds. To estimate  $T_{sf}$ , we have used the tight binding approximation of Harrison to calculate the hybridization  $V_{pf}$  between the Ce (or Pu)  $f$ -electrons and In (or Ga)  $p$ -electrons and  $V_{df}$  between the Ce  $f$ -electrons and  $M$  atom  $d$ -electrons. As  $T_{sf} \propto \exp(-1/V^2)$ , the hybridization can be directly linked to  $T_{sf}$ . It can be shown that the  $pf$  and  $df$  hybridization are given by

$$V_{pf} = \eta_{pf} \frac{\hbar^2 \sqrt{r_p r_f^5}}{m_e d^5}, \quad (2)$$

$$V_{df} = \eta_{df} \frac{\hbar^2 \sqrt{r_d^3 r_f^5}}{m_e d^6},$$

where  $\eta$  is a constant (for  $\sigma$  bonds,  $\eta_{pf} = 10\sqrt{21}/\pi$ ,  $\eta_{df} = 450\sqrt{35}/\pi$ );  $m_e$  is the mass of an electron;  $r_p$ ,  $r_d$ , and  $r_f$  are tabulated electron wave function radii for a particular atom;

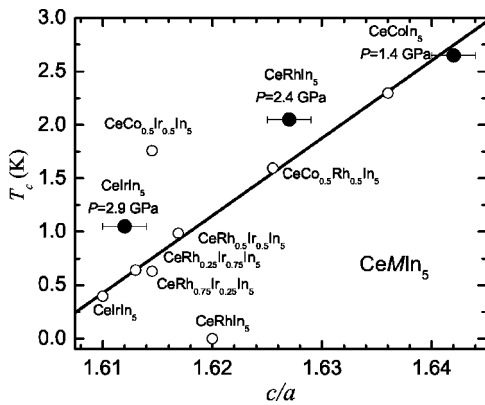


FIG. 4. The ambient pressure values of the superconducting transition temperature versus the room temperature value of  $c/a$  (open circles) for various  $CeMIn_5$  compounds. Also shown (solid circles) are the values of  $c/a$  determined at room temperature at the pressure  $P_{\max}$  where  $T_c(P)$  displays a maximum. The line is a least squares fit to the ambient pressure values.

TABLE II. Calculated  $fp$  ( $V_{fp}$ ) and the  $df$  ( $V_{df}$ ) hybridization in eV as described in text. Values are given at ambient pressure and the pressure where  $T_c$  displays a maximum  $P_{max}$ . Necessary structural parameters for  $PuCoGa_5$  are taken from Wastin *et al.* (Ref. 44) and for  $Ce_2CoIn_8$  from Kalychak *et al.* (Ref. 45).

System	$V_{df}(0)$	$V_{pf}(0)$	$P_{max}$ (GPa)	$V_{df}(P_{max})$	$V_{pf}(P_{max})$
$CeRhIn_5$	0.572	2.030	2.4	0.607	2.136
$CeIrIn_5$	0.627	2.031	2.9	0.665	2.135
$CeCoIn_5$	0.307	2.066	1.4	0.317	2.130
$Ce_2RhIn_8$	0.272	1.977	2.4	0.292	2.086
$Ce_2IrIn_8$	0.297	1.993			
$Ce_2CoIn_8$	0.147	2.018			
$PuCoGa_5$	0.955	5.229			

and  $d$  is the distance between the atoms in question.<sup>40–43</sup> We tabulate ambient pressure values along with values at the pressure where  $T_c$  reaches its maximum value  $P_{max}$  of both the  $fp$  ( $V_{fp}$ ) and the  $df$  ( $V_{df}$ ) hybridization, summing over all nearest neighbors, in Table II. Note that though we have done the calculation only for  $\sigma$  bonds, the inclusion of bonding with higher  $m$  quantum numbers will simply multiply the final result by a constant (that should approximately be the same for all members of an isostructural series). From Table II, it is evident that  $V_{pf} > V_{df}$  for all of the compounds. This is consistent with the electronic structure calculations of Maehira *et al.* that consider the  $fp$  hybridization only and get good agreement to measured Fermi surfaces.<sup>46</sup> This dominance of the  $fp$  hybridization also gives a natural explanation to some facts regarding the robustness of superconductivity. For  $M$  site substitution, superconductivity is robust and exists for numerous  $CeMIn_5$  compositions.<sup>20,47</sup> Substitution of Sn for In, however, has been shown to rapidly suppress superconductivity in  $CeCo(In_{1-x}Sn_x)_5$ .<sup>48</sup> These results show that the  $M$  atom serves mainly to affect the spacing between the Ce and In atoms that determine the hybridization, and the sensitivity to Sn substitution shows that disorder of the Ce-In strongly perturbs the  $pf$  interactions leading to superconductivity.

For the  $CeMIn_5$  series, the  $V_{pf}$  values increase in the order  $Rh \rightarrow Ir \rightarrow Co$ . One expects the important parameter describing the magnetic interaction to be the magnetic coupling  $J \propto V^2$ . This is consistent with a Doniach model<sup>49,50</sup> of the competition between the nonmagnetic Kondo state and the magnetic RKKY state shown schematically in Fig. 5 which qualitatively captures the pressure dependent behavior in  $CeMIn_5$  compounds. After a system has reached its maximum magnetic ordering temperature, the magnetic order is rapidly suppressed and the system moves toward a QCP. This type of behavior has been seen in numerous Ce compounds.<sup>51–53</sup> Near the QCP, many different behaviors can be observed. For the  $CeMIn_5$  compounds, superconductivity with a characteristic inverse parabolic shape is observed. As shown by the dotted line, magnetic order may or may not coexist in regions with superconductivity. In Fig. 5, the compounds were placed from left to right in order of increasing

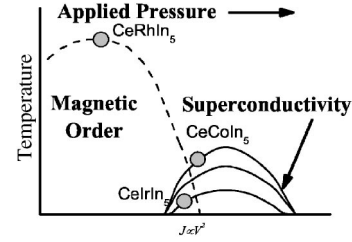


FIG. 5. Schematic phase diagram for the  $CeMIn_5$  compounds showing the competition between magnetic order and superconductivity. For small values of the hybridization  $V^2$ , the magnetically ordered state (dashed line) is favored. As pressure is applied, systems move to the right in the diagram and the magnetically ordered state gives away to superconductivity (solid lines). The approximate ambient pressure position is shown for various  $CeMIn_5$  materials. The superconducting curve for  $CeRhIn_5$  lies between the  $CeIrIn_5$  and  $CeCoIn_5$  curves.

$V_{pf}$ . The location was chosen to agree with the measured behavior of all three compounds. Namely,  $CeRhIn_5$  is an antiferromagnet at ambient pressure while  $CeIrIn_5$  and  $CeCoIn_5$  are ambient pressure superconductors, and all three display a maximum in  $T_c$  as a function of pressure. The inverse parabolic shape of  $T_c$  is consistent with the behavior expected for magnetically mediated superconductivity, where the height of the maximum depends on the hybridization and the dimensionality.<sup>21</sup> The larger maximum value of  $T_c$  as a function of pressure for  $CeCoIn_5$  with larger  $c/a$  (and hence more 2D character) relative to  $CeIrIn_5$  then follows naturally. From Fig. 5, one would expect that the pressure to reach the maximum in  $T_c$  would increase in order  $Rh \rightarrow Ir \rightarrow Co$ . Surprisingly, both Rh and Ir display the maximum at about the same pressure of 2.4 GPa. This can be explained, however, by noting that  $CeIrIn_5$  has the larger bulk modulus so that while the pressure is the same, the volume change is considerably less. A more reasonable variable to use than pressure would be the hybridization  $V$ . From Table II, the value for the hybridization at the pressure  $P_{max}$  where  $T_c$  reaches its maximum value is nearly identical for all three  $CeMIn_5$  compounds. This gives strong support for the magnetically mediated superconductivity scenario as one would expect that the maximum value of  $T_c$  would occur for approximately the same value of  $V$  and variations in  $T_c$  would then be attributed to differences in dimensionality. We note that the values of  $V_{pf}$  for the  $Ce_2MIn_8$  compounds is very similar to the  $CeMIn_5$  compounds and the progression of increasing  $V_{pf}$  being  $Rh \rightarrow Ir \rightarrow Co$ ; this is consistent with the progression of ground states from magnetic order (Rh) to heavy fermion (Ir) to superconductivity (Co) in the  $Ce_2MIn_8$  series. This is in line with the experimental finding of very similar electronic specific heat coefficients  $\gamma \propto 1/T_{sf} \propto \exp(1/V^2)$ .<sup>24,54,55</sup> Also, in a scenario of magnetically mediated superconductivity, the most obvious route to higher  $T_c$  values would be to raise the value of  $T_{sf}$  by switching to actinide compounds with larger  $r_f$  values, and hence hybridization relative to rare earths. The affect of moving to the actinides is seen in  $PuCoGa_5$  that has  $V_{pf} \sim 2.6$  times larger than the corresponding Ce compounds.

Recently, Pu based superconductivity was observed for the first time in  $PuCoGa_5$  above 18 K, an order of magnitude

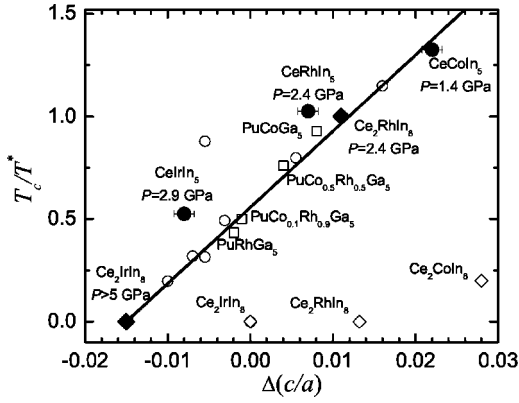


FIG. 6. The ambient pressure values of  $T_c/T^*$  versus the room temperature value of  $\Delta(c/a)$  (open symbols) for various  $\text{Ho}_n\text{CeGa}_{2n+3}$  based compounds;  $\text{CeMIn}_5$  (circles),  $\text{Ce}_2\text{MIn}_8$  (diamonds), and  $\text{PuMGa}_5$  (squares) are all shown. Also shown (solid symbols) are the values of  $\Delta(c/a)$  determined at room temperature at the pressure  $P_{\text{max}}$  where  $T_c(P)$  displays a maximum. The straight line is the same as that shown in Fig. 4.

larger than the Ce compounds that also have the  $\text{HoCoGa}_5$  structure.<sup>56</sup> It was subsequently shown by Wastin *et al.* that a similar universal linear behavior of  $T_c$  versus  $c/a$  is observed in  $\text{PuMGa}_5$  compound with nearly the same logarithmic slope as the  $\text{CeMIn}_5$  compounds.<sup>44,57</sup> While this may at first seem a surprising result, in fact it follows straight from the theoretical conclusions that  $T_c$  should scale as a characteristic temperature  $T^* \propto T_{sf}$ . That the value  $T_c$  is an order of magnitude larger in Pu based compared to Ce based compounds then is a consequence of a value of  $T_{sf}$  that is an order of magnitude larger in Pu compounds. This estimate is reasonable in light of the previous discussion showing a significantly larger value of  $V_{pf}$  in the Pu compounds remembering that  $T_{sf} \propto \exp(-1/V^2)$ , and also because the electronic specific heat coefficient  $\gamma$  is an order of magnitude smaller in Pu compounds relative to Ce compounds and  $T_{sf} \propto 1/\gamma$ .<sup>56</sup> We also note that the  $\text{Ce}_2\text{MIn}_8$  compounds at ambient pressure do not seem to not follow the linear  $T_c$  versus  $c/a$  behavior as only  $\text{Ce}_2\text{CoIn}_8$  displays superconductivity at ambient pressure. However,  $\text{Ce}_2\text{RhIn}_8$ , like  $\text{CeRhIn}_5$ , magnetically orders at ambient pressure but the application of pressure reveals superconductivity. To further analyze these systems, we plot normalized values of  $T_c$  versus  $\Delta(c/a)$  in Fig. 6, where  $T_c$  is normalized by  $T^*$  and  $\Delta(c/a)$  is found by subtracting a value  $(c/a)^*$ .  $T^*$  was chosen as 2 K for  $\text{CeMIn}_5$  and  $\text{Ce}_2\text{MIn}_8$  as it is approximately  $T_{sf}$  for  $\text{CeCoIn}_5$ ,<sup>58</sup> and as discussed previously, we do not expect much variation in  $T_{sf}$  for these compounds.  $T^* = 20$  K was used for  $\text{PuMGa}_5$  as we expect an order of magnitude increase in  $T_{sf}$  for Pu compounds relative to Ce compounds.  $(c/a)^*$  was chosen in such a way to shift the curves on top of each other. The values of  $T^*$  and  $(c/a)^*$  are given in Table III. The normalized values are plotted in Fig. 6. The universality is readily apparent with all of the pressure points lying on or above the straight line. That the points lie on or above the line for the ambient pressure points is likely due to higher values of  $T_{sf}$  for the optimal pressure data relative to ambient pressure data rendering the assumption of a single  $T^*$  value to normalize all data tenuous. The

TABLE III. Summary of the normalization values used to plot the data in Fig. 6.  $T^*$  is a characteristic temperature that is related to the spin fluctuation or Kondo temperature.  $(c/a)^*$  is chosen as described in text.

System	$T^*$ (K)	$(c/a)^*$
$\text{CeMIn}_5$	2.0	1.620
$\text{PuMGa}_5$	20	1.596
$\text{Ce}_2\text{MIn}_8$	2.0	2.610

ambient pressure “misplacement” of  $\text{Ce}_2\text{RhIn}_8$  (AF order at ambient pressure) now can be explained by the pressure induced superconductivity and the universal line now goes through the high pressure  $\text{Ce}_2\text{MIn}_8$  data. While  $\text{Ce}_2\text{IrIn}_8$  does not display superconductivity, the value of  $c/a$  reaches a nearly constant value above 5 GPa and we have plotted a point assuming  $T_c = 0$  at high pressure. This assumption gains validity as these results would predict that superconductivity will not be seen in  $\text{Ce}_2\text{IrIn}_8$  under pressure as  $\Delta(c/a)$  falls below the x-intercept of the  $T_c/T^*$  versus  $\Delta(c/a)$  line. Also,  $\text{Ce}_2\text{CoIn}_8$  should see a dramatic enhancement of  $T_c$  under pressure; if  $c/a$  doesn’t change as a function of pressure, this estimate for the maximum in  $T_c$  would be around 3 K which is slightly larger than what is seen in  $\text{CeCoIn}_5$  under pressure.

#### IV. CONCLUSIONS

We have studied the elastic properties of  $\text{Ce}_n\text{MIn}_{2n+3}$  ( $M = \text{Rh, Ir, and Co}$ ) with  $n = 1$  or 2 under hydrostatic and quasi-hydrostatic pressures up to 15 GPa using x-ray diffraction. The addition of  $\text{MIn}_2$  layers to the parent  $\text{CeIn}_3$  compound is found to stiffen the lattice. By plotting the maximum values of the superconducting transition temperature  $T_c$  versus  $c/a$ , we are able to expand upon the proposed linear relationship between the quantities by Pagliuso *et al.*<sup>20</sup> We have also found that the dominant hybridization is between the Ce (or Pu)  $f$ -electrons and In (or Ga)  $p$ -electrons  $V_{pf}$ . Also, the value of  $V_{pf}$  where  $T_c$  reaches its maximum is nearly identical for all three  $\text{CeMIn}_5$  compounds. These results explain the lack of superconductivity in  $\text{Ce}_2\text{IrIn}_8$  and predict that  $T_c$  should increase dramatically in  $\text{Ce}_2\text{CoIn}_8$  at high pressure. Comparing the results to Pu-based superconductors shows a universal  $T_c$  versus  $c/a$  behavior when these quantities are normalized by appropriate quantities consistent with what is expected of magnetically mediated superconductivity.

#### ACKNOWLEDGMENTS

Work at UNLV is supported by DOE EPSCoR-State/National Laboratory Partnership Grant No. DE-FG02-00ER45835. Work at LANL is performed under the auspices of the U.S. Department of Energy. HPCAT is a collaboration among the UNLV High Pressure Science and Engineering Center, the Lawrence Livermore National Laboratory, the Geophysical Laboratory of the Carnegie Institution of

Washington, and the University of Hawaii at Manoa. The UNLV High Pressure Science and Engineering Center was supported by the U.S. Department of Energy, National Nuclear Security Administration, under Cooperative Agree-

ment DE-FC08-01NV14049. Use of the Advanced Photon Source was supported by the U.S. Department of Energy, Office of Science, Office of Basic Energy Sciences, under Contract No. W-31-109-Eng-38.

- <sup>1</sup>F. Steglich, J. Aarts, C. D. Bredl, W. Lieke, D. Meschede, W. Franz, and H. Schäfer, *Phys. Rev. Lett.* **43**, 1892 (1979).
- <sup>2</sup>D. Jaccard, K. Behina, and J. Sierro, *Phys. Lett. A* **163**, 475 (1992).
- <sup>3</sup>R. Movshovich, T. Graf, D. Mandrus, J. D. Thompson, J. L. Smith, and Z. Fisk, *Phys. Rev. B* **53**, 8241 (1996).
- <sup>4</sup>F. M. Grosche, S. R. Julian, N. D. Mathur, and G. G. Lonzarich, *Physica B* **223–224**, 50 (1996).
- <sup>5</sup>N. D. Mathur, F. M. Grosche, S. R. Julian, I. R. Walker, D. M. Freye, R. K. Haselwimmer, and G. G. Lonzarich, *Nature (London)* **394**, 39 (1998).
- <sup>6</sup>Y. N. Grin, Y. P. Yarmolyuk, and E. I. Gladyshevskii, *Sov. Phys. Crystallogr.* **24**, 137 (1979).
- <sup>7</sup>Y. N. Grin, P. Rogl, and K. Hiebl, *J. Less-Common Met.* **121**, 497 (1986).
- <sup>8</sup>J. M. Lawrence and S. M. Shapiro, *Phys. Rev. B* **22**, 4379 (1980).
- <sup>9</sup>A. L. Cornelius, A. J. Arko, J. L. Sarrao, M. F. Hundley, and Z. Fisk, *Phys. Rev. B* **62**, 14 181 (2000).
- <sup>10</sup>N. J. Curro, P. C. Hammel, P. G. Pagliuso, J. L. Sarrao, J. D. Thompson, and Z. Fisk, *Phys. Rev. B* **62**, R6100 (2000).
- <sup>11</sup>W. Bao, P. G. Pagliuso, J. L. Sarrao, J. D. Thompson, Z. Fisk, J. W. Lynn, and R. W. Erwin, *Phys. Rev. B* **62**, R14 621 (2000).
- <sup>12</sup>H. Hegger, C. Petrovic, E. G. Moshopoulou, M. F. Hundley, J. L. Sarrao, Z. Fisk, and J. D. Thompson, *Phys. Rev. Lett.* **84**, 4986 (2000).
- <sup>13</sup>R. A. Fisher, F. Bouquet, N. E. Phillips, M. F. Hundley, P. G. Pagliuso, J. L. Sarrao, Z. Fisk, and J. D. Thompson, *Phys. Rev. B* **65**, 224509 (2002).
- <sup>14</sup>T. Mito, S. Kawasaki, G. q. Zheng, Y. Kawasaki, K. Ishida, Y. Kitaoka, D. Aoki, Y. Haga, and Y. Onuki, *Phys. Rev. B* **63**, 220507(R) (2001).
- <sup>15</sup>M. Nicklas, V. A. Sidorov, H. A. Borges, P. G. Pagliuso, C. Petrovic, Z. Fisk, J. L. Sarrao, and J. D. Thompson, *Phys. Rev. B* **67**, 020506 (2003).
- <sup>16</sup>C. Petrovic, P. G. Pagliuso, M. F. Hundley, R. Movshovich, J. L. Sarrao, J. D. Thompson, Z. Fisk, and P. Monthoux, *J. Phys.: Condens. Matter* **13**, L337 (2001).
- <sup>17</sup>C. Petrovic, R. Movshovich, M. Jaime, P. G. Pagliuso, M. F. Hundley, J. L. Sarrao, Z. Fisk, and J. D. Thompson, *Europhys. Lett.* **53**, 354 (2001).
- <sup>18</sup>G. Chen, S. Ohara, M. Hedo, Y. Uwatoko, K. Saito, M. Sorai, and I. Sakamoto, *J. Phys. Soc. Jpn.* **71**, 2836 (2002).
- <sup>19</sup>J. D. Thompson *et al.*, *J. Magn. Magn. Mater.* **226**, 5 (2001).
- <sup>20</sup>P. G. Pagliuso, R. Movshovich, A. D. Bianchi, M. Nicklas, N. O. Moreno, J. D. Thompson, M. F. Hundley, J. L. Sarrao, and Z. Fisk, *Physica B* **312–313**, 129 (2002).
- <sup>21</sup>P. Monthoux and G. G. Lonzarich, *Phys. Rev. B* **63**, 054529 (2001).
- <sup>22</sup>R. S. Kumar, H. Kohlmann, B. E. Light, A. L. Cornelius, V. Raghavan, T. W. Darling, and J. L. Sarrao, *Phys. Rev. B* **69**, 014515 (2004).
- <sup>23</sup>E. G. Moshopoulou, Z. Fisk, J. L. Sarrao, and J. D. Thompson, *J. Solid State Chem.* **158**, 25 (2001).
- <sup>24</sup>N. O. Moreno, M. F. Hundley, P. G. Pagliuso, R. Movshovich, M. Nicklas, J. D. Thompson, J. L. Sarrao, and Z. Fisk, *Physica B* **312–313**, 274 (2002).
- <sup>25</sup>A. P. Hammersley, S. O. Svensson, M. Hanfland, A. N. Fitch, and D. Häusermann, *High Press. Res.* **14**, 235 (1996).
- <sup>26</sup>J. Rodriguez-Carvajal, *Physica B* **192**, 55 (1993).
- <sup>27</sup>J. M. Brown, *J. Appl. Phys.* **86**, 5801 (1999).
- <sup>28</sup>G. J. Piermarini, S. Block, J. D. Barnett, and R. A. Forman, *J. Appl. Phys.* **46**, 2774 (1975).
- <sup>29</sup>I. Vedel, A. M. Redon, J. M. Mignot, and J. M. Leger, *J. Phys. F: Met. Phys.* **17**, 849 (1987).
- <sup>30</sup>T. Penney, B. Barbara, T. S. Plaskett, H. E. J. King, and S. J. LaPlaca, *Solid State Commun.* **44**, 1199 (1982).
- <sup>31</sup>I. L. Spain, F. Steglich, U. Rauchschwalbe, and H. D. Hochheimer, *Physica B* **139–140**, 449 (1986).
- <sup>32</sup>A. P. G. Kutty and S. N. Vaidya, in *Theoretical and Experimental Aspect of Valence Fluctuations and Heavy Fermions*, edited by L. C. Gupta and S. K. Malik (Plenum, New York, 1987), p. 621.
- <sup>33</sup>C. Wassilew-Reul, M. Kunz, M. Hanfland, D. Häusermann, C. Geibel, and F. Steglich, *Physica B* **230–232**, 310 (1997).
- <sup>34</sup>V. A. Sidorov, M. Nicklas, P. G. Pagliuso, J. L. Sarrao, Y. Bang, A. V. Balatsky, and J. D. Thompson, *Phys. Rev. Lett.* **89**, 157004 (2002).
- <sup>35</sup>G. Sparn, R. Borth, E. Lengyel, P. G. Pagliuso, J. L. Sarrao, F. Steglich, and J. D. Thompson, *Physica B* **319**, 262 (2002).
- <sup>36</sup>T. Muramatsu, T. C. Kobayashi, K. Shimizu, K. Amaya, D. Aoki, Y. Haga, and Y. Onuki, *Physica C* **388–389**, 539 (2003).
- <sup>37</sup>P. Monthoux and G. G. Lonzarich, *Phys. Rev. B* **69**, 064517 (2004).
- <sup>38</sup>T. Muramatsu, N. Tateiwa, T. C. Kobayashi, A. Shimizu, K. Amaya, D. Aoki, H. Shishido, Y. Haga, and Y. Onuki, *J. Phys. Soc. Jpn.* **70**, 3362 (2001).
- <sup>39</sup>M. Nicklas, V. A. Sidorov, H. A. Borges, P. G. Pagliuso, J. L. Sarrao, and J. D. Thompson, *Phys. Rev. B* **70**, 020505(R) (2004).
- <sup>40</sup>W. A. Harrison, *Electronic Structure and the Properties of Solids* (Freeman, San Francisco, 1980).
- <sup>41</sup>W. A. Harrison, *Phys. Rev. B* **28**, 550 (1983).
- <sup>42</sup>G. K. Straub and W. A. Harrison, *Phys. Rev. B* **31**, 7668 (1985).
- <sup>43</sup>W. A. Harrison and G. K. Straub, *Phys. Rev. B* **36**, 2695 (1987).
- <sup>44</sup>F. Wastin, P. Boulet, J. Rebizant, E. Colineau, and G. H. Lander, *J. Phys.: Condens. Matter* **15**, S2279 (2003).
- <sup>45</sup>Y. M. Kalychak, V. I. Zaremba, V. M. Baranyak, V. A. Bruskov, and P. Y. Zavalii, *Izv. Akad. Nauk. SSSR, Met.* **1**, 209 (1989).
- <sup>46</sup>T. Maehira, T. Hotta, K. Ueda, and A. Hasegawa, *J. Phys. Soc. Jpn.* **72**, 854 (2003).
- <sup>47</sup>P. G. Pagliuso, C. Petrovic, R. Movshovich, D. Hall, M. F. Hundley, J. L. Sarrao, J. D. Thompson, and Z. Fisk, *Phys. Rev. B* **64**, 100503(R) (2001).

- <sup>48</sup>E. D. Bauer (private communication).
- <sup>49</sup>S. Doniach, in *Valence Instability and Related Narrow Band Phenomena*, edited by R. D. Parks (Plenum, New York, 1977).
- <sup>50</sup>S. Doniach, *Physica B* **231–234**, 231 (1977).
- <sup>51</sup>J. D. Thompson and J. M. Lawrence, *Handbook on the Physics and Chemistry of Rare Earths* (North-Holland, Amsterdam, 1994), Vol. 19, Chap. 133, pp. 383–477.
- <sup>52</sup>A. L. Cornelius and J. S. Schilling, *Phys. Rev. B* **49**, 3955 (1994).
- <sup>53</sup>A. L. Cornelius, A. K. Gangopadhyay, J. S. Schilling, and W. Assmus, *Phys. Rev. B* **55**, 14 109 (1997).
- <sup>54</sup>A. L. Cornelius, P. G. Pagliuso, M. F. Hundley, and J. L. Sarrao, *Phys. Rev. B* **64**, 144411 (2001).
- <sup>55</sup>J. D. Thompson *et al.*, *Physica B* **329**, 446 (2003).
- <sup>56</sup>J. L. Sarrao, L. A. Morales, J. D. Thompson, B. L. Scott, G. R. Stewart, J. R. F. Wastin, P. Boulet, E. Colineau, and G. H. Lander, *Nature (London)* **420**, 297 (2002).
- <sup>57</sup>F. Wastin, P. Boulet, E. Colineau, J. Rebizant, G. H. Lander, J. D. Thompson, J. L. Sarrao and L. A. Morales (unpublished).
- <sup>58</sup>S. Nakatsuji, S. Yeo, L. Balicas, Z. Fisk, P. Schlottmann, P. G. Pagliuso, N. O. Moreno, J. L. Sarrao, and J. D. Thompson, *Phys. Rev. Lett.* **89**, 106402 (2002).